DEFENCE R&D DÉFENSE

In-Situ Calibration of an X-Band Antenna Array for Low-Angle Tracking with High-Resolution Direction-Finding Methods

Eric K.L. Hung
Defence Research Establishment Ottawa

Defence R&D Canada
DEFENCE RESEARCH ESTABLISHMENT OTTAWA

TECHNICAL MEMORANDUM
DREO TM 2000-122
November 2000

National Defence Défense nationale

Canada

DEFENCE R&D DÉFENSE

In-Situ Calibration of an X-Band Antenna Array for Low-Angle Tracking with High-Resolution Direction-Finding Methods

Eric K.L. Hung
Ground Based Radar Group
Surface Radar Section

DEFENCE RESEARCH ESTABLISHMENT OTTAWA

TECHNICAL MEMORANDUM
DREO TM 2000-122
November 2000

Project
05AB11

Abstract

Presented in this report is an in-situ method to calibrate X-band antenna arrays designed to detect and track low-level missiles over water. These arrays are indispensable in ship defence, because they can operate in rainy and foggy conditions where atmospheric absorption is too high for the use of more accurate millimetre wave radars or optical devices.

The method uses a set of array snapshots to construct a calibration matrix for the antenna array. It incorporates the compensations for unequal gain and phase responses at the array elements, antenna tilt, mutual coupling among the elements, the effect of local structures, and small errors in element positions.

Simulation and experimental evaluations showed that the calibration (a) improved the accuracy of target elevation angle estimates obtained with a high-resolution direction-finding method, (b) improved the resolution of target and image elevation angles, (c) suppressed a bias in elevation angle estimates, and (d) suppressed some anomalous tracks between the true target and image tracks.

The calibration improves a ship's defence against low-level missiles.

Résumé

Ce rapport présente une méthode d'étalonnage sur place de réseaux d'antennes à bande X utilisées pour la détection et la poursuite de missiles volant à basse altitude au-dessus de l'océan. Ces réseaux sont indispensables pour la défense des navires, car ils peuvent opérer dans des conditions de pluie et de brouillard pour lesquelles l'atténuation atmosphérique est trop grande pour l'utilisation de radar millimétrique plus précis ou d'équipement optique.

La méthode utilise un ensemble de mesures instantanées du réseau pour construire une matrice d'étalonnage pour le réseau d'antennes. Elle incorpore une compensation pour les réponses inégalées en phases et gain au niveau des éléments du réseau, de l'inclinaison de l'antenne, du couplage mutuelle entre les éléments, pour les effets des structures locales, et des petites erreurs dans les positions des éléments.

Les évaluations expérimentales et simulées montrent que l'étalonnage (a) améliore la précision des mesures de l'angle de site des cibles obtenu avec une méthode de radiogoniométrie de haute résolution, (b) améliore la résolution des angles de site de la cible et de son image, (c) élimine une erreur sur la mesure des angles de site, et (d) élimine quelques anomalies entre les vraies pistes des cibles et leurs images.

L'étalonnage améliore la défense des navires contre les missiles volant à basses altitudes

This page intentionally left blank.

Executive summary

This report describes the in-situ calibration of X-band antenna arrays designed to detect and track low-level sea skimming missiles. X-band antenna arrays are indispensable in ship defence against these missiles, especially in foggy and rainy conditions where optical and millimetre wave radars become ineffective in detecting these targets.

The antenna arrays must be calibrated accurately, because a more accurately calibrated array yields a more accurate estimate of missile elevation. Practical considerations require the calibration be carried out in-situ with a remote pilot source. This report describes the first successful attempt to use this type of source in calibration.

Simulation and experimental evaluations showed that the calibration (a) improved the accuracy of target elevation angle estimates obtained with a high-resolution direction-finding method, (b) improved the resolution of target and image elevation angles, (c) suppressed a bias in elevation angle estimates, and (d) suppressed some anomalous tracks between the true target and image tracks.

The calibration method can be used to calibrate the ship-borne X-band Active Phased Array Radar (APAR) being jointly developed by Canada, Germany and the Netherlands.

Hung, Eric K.L. 2000. Defence Scientist. DREO TM-2000-122. DREO.

Sommaire

Ce rapport décris l'étalonnage sur place de réseaux d'antennes à bande X utilisée pour la détection et la poursuite de missiles volant à basse altitude au-dessus de l'océan. Les réseaux d'antennes à bande X sont indispensables à la défense des navires contre ces missiles, spécialement dans des conditions de pluie et de brouillard ou les instruments optique et les radar millimétriques sont inefficaces pour détecter ces cibles.

Le réseau d'antennes doit être précisément étalonner, car un réseau étalonner produit une mesure plus précise de l'angle de site des cibles Des considérations pratique exigent que l'étalonnage soit fait sur place avec une source pilote à distance. Ce rapport décris le premier essai réussi pour l'utilisation de ce type de source pour l'étalonnage.

Les évaluations expérimentales et simulées montrent que l'étalonnage (a) améliore la précision des mesures de l'angle de site des cibles obtenu avec une méthode de radiogoniométrie de haute résolution, (b) améliore la résolution des angles de site de la cible et de son image, (c) élimine une erreur sur la mesure des angles de site, et (d) élimine quelques anomalies entre les vraies pistes des cibles et leurs images.

La méthode d'étalonnage peut être utilisée pour étalonner les radars navals à antenne réseau active à bande X développée conjointement par le Canada, L'Allemagne, et les Pays-Bas.

Hung, Eric K.L. 2000. Defence Scientist. DREO TM-2000-122. DREO.

Table of contents

List of figures

List of tables

Acknowledgements

I would like to thank my former group leader, Dr. Ross M. Turner, for this assignment and his encouragement while he and the other authors in [11,13] were working on the RML method. The experimental data were measured by the Standard Telecommunications Laboratory and made available to the Canadian government in 1982 by the Admiralty Surface Weapons Establishment (now part of the Defence Evaluation and Research Agency), United Kingdom, under the auspices of the The Technical Cooperation Program. This work was funded by the Department of National Defence, Canada.

This page intentionally left blank.

1. Introduction

X-band antennas are indispensable in ship defence against low-elevation missiles. These antennas can operate in rainy and foggy conditions where atmospheric absorption is too high for the use of more accurate optical devices or millimetre wave radars.

Low-angle tracking (LAT) methods for X-band antenna arrays must deal with the presence of interfering image signals produced by reflections off the water surface. They can be divided into two groups. The first group uses established high-resolution direction-finding (HRDF) methods such as the MUSIC method [1] and the Tufts-Kumaresan singular value decomposition (TKSVD) method [2,3] to estimate target elevation angles. An example of application is given by Haykin, Greenlay and Litva in [4]. The second group comprises several maximum likelihood estimation (MLE) methods. It includes (i) the Correlation Height Analysis (CHA) method and its variants [5-10] developed by Litva, Rook, Lo and Wong and (ii) the refined maximum likelihood (RML) method developed by Bosse, Turner, Lecours, Brookes and Riseborough [11,13]. These MLE methods use a highly deterministic model of the propagation medium to model the interference pattern of the target and image signals at the array. The target height estimate is the height that produces the best match between the modelled and measured patterns. Target elevation angle is derived from the target height. Based on the results presented, the MLE methods are overwhelmingly superior to the HRDF methods. In particular, they produce extremely accurate estimates of target heights and elevation angles. They are also very tolerant to inadequacies in array calibration.

The MLE methods require the development of a practical propagation model that can produce the true target-plus-image component of the measured interference pattern at the array elements. This task is difficult, because the above component changes with time and it is not always possible to measure many key parameters, e.g. temperature and moisture gradients at the water surface, in battlefield conditions.

HRDF methods do not need a propagation model. However, they require a reasonably accurately calibrated antenna array for implementation in LAT systems. The calibration is required to compensate for unequal gain and phase responses at the array elements, antenna tilt, mutual coupling among the elements, the effect of the ship=s structure, and small errors in element positions. Some negative effects of calibration errors on direction estimates have been discussed by Friedlander [14,15].

Several factors influence the design of calibration methods for LAT arrays. Firstly, an off-site calibration still requires an on-site refinement. The off-site calibration cannot compensate for antenna tilt and the effect of the ship=s structure. Besides, the process of moving the antenna to a ship may change the relative gain and phase responses at the array elements. Secondly, for an on-site refinement with a near-field source, the effect of the ship=s structures differs from what it would be with true targets many kilometres from the ships. Finite source size and errors in effective element positions may also introduce errors in the equalisation of element gain and phase responses. Thirdly, for a refinement with a fixed distant pilot source, the target and image signals produce an interference pattern that changes with time.

The antenna calibration methods in [5-13] were not designed for HRDF methods. In [8] and [10], for example, Lo and Litva only ensured accurate alignment of element positions in the field. In [12] and [13], Bosse, Turner, Brookes and Riseborough used a calibration source 4.6 km from the antenna array. They used the statistical average of sea-state 5 data to refine the gain responses. The authors did not refine the phase responses.

An effective in-situ method to refine the calibration of a LAT antenna array is presented here. The method is derived from a matrix calibration method developed by Hung [16,17]. It requires a large number of array snapshots generated by moving a remote pilot source over the range of target elevation angles covered by the array. In evaluations with a HRDF method, the calibration improved the accuracy of target elevation angle estimates, improved the resolution of target and image elevation angles, suppressed a bias in elevation angle estimates, and suppressed some anomalous tracks between the true target and image tracks.

In the following discussions, Section 2 describes the new calibration method, Sections 3 and 4 evaluate the method with simulated and experimental data, respectively, and Section 5 contains the conclusions.

2. Calibration method

The calibration method requires reasonably accurate elevation angles of the target and image signals in the array snapshots. A method to calculate the image elevation angles will be presented in the analysis of experiment data. The following contains a brief description of the signal model used, the assumptions made, and the computational procedure.

2.1 Signal model

There are N array elements. The m-th ideal array snapshot is given by

$$\mathbf{x}_m = \alpha_{Tm}\mathbf{a}(\theta_{Tm}) + \alpha_{Im}\mathbf{a}(\theta_{Im}) , \tag{1}$$

where α_{Tm} and α_{Im} are the complex amplitudes of the received target and image signals, respectively, θ_{Tm} and θ_{Im} are the target and image signal elevation angles, and $\mathbf{a}(\theta_{Tm})$ and $\mathbf{a}(\theta_{Im})$ are the array steering vectors for θ_{Tm} and θ_{Im}. This expression assumes a perfectly calibrated array, a pure tone signal source, no interaction among the array elements, no noise, and no interference besides the image signal.

The corresponding measured array snapshot is given by $\mathbf{y}_m$, with

$$\mathbf{y}_m = \mathbf{B}\mathbf{x}_m + \mathbf{e}_m . \tag{2}$$

Matrix **B** has dimension NHN and depends on the gain and phase responses at the array elements, antenna tilt, mutual coupling among the elements, the effect of the ship=s structure, and errors in element positions. The vector $\mathbf{e}_m$ denotes the sum of noise and unknown interfering signals.

Let $\{\mathbf{y}_1,\mathbf{y}_2,AAA,\mathbf{y}_M\}$ be a set of M array snapshots. The calibration matrix calculated with these snapshots is identified here as the NHN matrix C that minimises the objective function

$$S = \sum_{m=1}^{M} *\mathbf{C}\mathbf{y}_m - \hat{\mathbf{x}}_m *^2 \Big/ \sum_{m=1}^{M} *\mathbf{C}\mathbf{y}_m *^2, \tag{3}$$

subject to the uniqueness condition

$$C_{11} = 1.0 . \tag{4}$$

The $\hat{\mathbf{x}}_m$ is a component of $\mathbf{C}\mathbf{y}_m$ and the division by the sum of $*\mathbf{C}\mathbf{y}_m*^2$ is designed to cancel the effect of an unknown scaling factor introduced by **C**. Matrix **C** is proportional to $\mathbf{B}^{-1}$ if each $\mathbf{e}_m$ is a null vector.

In the convention used, >^= denotes an estimate, superscript >H= denotes a conjugate-transpose, the set $\{C_{pq}: p,q=1,2,\cong\cong\cong,N\}$ denotes the coefficients of matrix **C**, and $\mathbf{y}_m^c$, defined as

$$\mathbf{y}_m^c = \mathbf{C}\mathbf{y}_m \,, \tag{5}$$

denotes a calibrated snapshot.

2.2 Conditions

The following conditions are assumed to be satisfied:

1. The array elements are narrowband;

2. The process that converts an ideal array snapshot to a measured snapshot can be approximated by a matrix operation;

3. The calibration data are generated by moving a remote pilot source over the range of elevation angles covered by the antenna array;

4. There are many array snapshots in the calibration data;

5. The target elevation angles are given; and

6. A preliminary calibration has been carried out, so that one can obtain reasonably accurate estimates of the image elevation angles from the calibration data by curve fitting.

Conditions 3 and 4 are needed for tolerance to noise, unknown interference, and unknowns in the propagation medium. One can assume that Condition 4 is satisfied if, say, every fifth snapshot in the calibration data is deleted and the new calibration matrix **C**= is essentially the same as **C**, so that $\mathbf{C}^{-1}\mathbf{C}$= is approximately a constant times $\mathbf{I}_N$.

2.3 Computation of calibration matrix

The calculation of calibration matrix **C** is based on the observations presented below.

A. Matrix **C** must be calculated iteratively, yielding a sequence $\{\mathbf{C}_0,\mathbf{C}_1,\mathbf{C}_2,AAA\}$, where $\mathbf{C}_0$ is the initial estimate of **C**.

B. Let $\mathbf{C}_{i-1}$ be an estimate of **C**, $\{\mathbf{u}_{1m},\mathbf{u}_{2m}\}$ be an orthonormal basis constructed from the array steering vectors $\mathbf{a}(\theta_{Tm})$ and $\mathbf{a}(\theta_{Im})$, and

$$\mathbf{z}_m = \mathbf{C}_{i-1}\mathbf{y}_m \,. \tag{6}$$

One can calculate an estimate of $\mathbf{x}_m$ as the component of $\mathbf{z}_m$ in the signal subspace spanned by $\mathbf{a}(\theta_{Tm})$ and $\mathbf{a}(\theta_{Im})$, i.e.

$$\hat{\mathbf{x}}_m = (\mathbf{u}_{1m}^H \mathbf{z}_m)\mathbf{u}_{1m} + (\mathbf{u}_{2m}^H \mathbf{z}_m)\mathbf{u}_{2m} . \quad (7)$$

C. Given the NHM data matrices $\hat{\mathbf{X}}$ and $\mathbf{Y}$, where $\hat{\mathbf{X}}=(\hat{\mathbf{x}}_1,\hat{\mathbf{x}}_2,AAA,\hat{\mathbf{x}}_M)$ and $\mathbf{Y}=(\mathbf{y}_1,\mathbf{y}_2,AAA,\mathbf{y}_M)$, one can estimate a new $\mathbf{C}$ which results in a smaller value of the objective function S by solving the equation

$$\mathbf{C}_i\mathbf{Y} = \hat{\mathbf{X}} \quad (8)$$

as

$$\mathbf{C}_i = (\hat{\mathbf{X}}\hat{\mathbf{X}}^H)(\mathbf{Y}\hat{\mathbf{X}}^H)^{-1} \quad (9)$$

and then impose the uniqueness condition given by Eq. (4) on $\mathbf{C}_i$.

D. The initialisation

$$\mathbf{C}_0 = \mathbf{I}_N , \quad (10)$$

where $\mathbf{I}_N$ is an NHN identity matrix, is equivalent to using the original data in the first iteration, i.e. $\mathbf{z}_m=\mathbf{y}_m$.

E. Let

$$\mathbf{D}_i = \mathbf{C}_i - \mathbf{C}_{i-1} \quad (11)$$

and

$$\Delta_i = \max\{*D_{pq}*: p,q=1,2,AAA,N\} . \quad (12)$$

One can terminate the iteration if (a) $\Delta_i<\Delta=$, where $\Delta=$ is a prespecified small value, or (b) $i>i_{max}$, where i_{max} is the maximum number of iterations specified.

F. If the objective function has more than one minimum, the matrix $\mathbf{C}_i$ that gives the smallest value of S is the desired $\mathbf{C}$.

The following procedure to calculate $\mathbf{C}$ is based on the above observations. There are seven steps.

Step 1.

Assign i_{max} and $\Delta=$.
Let i=1 and $\mathbf{C}_0=\mathbf{I}_N$.

Step 2.

For m=1,2, AAA,M
(a) calculate $\mathbf{z}_m$ with (6),

(b) calculate $\{\mathbf{u}_{1m},\mathbf{u}_{2m}\}$ with the Gram-Schmidt orthonormalization method

(c) calculate $\hat{\mathbf{x}}_m$ with (7).

Step 3

Calculate the value of S in the (i-1)th iteration with (3).

Step 4.

Calculate $\mathbf{C}_i$ with (9).
Impose the uniqueness condition (4) on $\mathbf{C}_i$.

Step 5.

Calculate Δ_i with (11) and (12).

Step 6.

If $\Delta_i<\Delta=$ or $i>i_{max}$,
Terminate the iterations and let $\mathbf{C}=\mathbf{C}_i$.
Else,
Replace i by i+1 and return to Step 2.

Step 7.

Repeat Steps 2 to 6 with many other initial values of $\mathbf{C}_0$. Study the values of S and the coefficients in C as well as the dependence of S and $\mathbf{C}_i$ on $\mathbf{C}_0$. Identify the $\mathbf{C}_i$ with the overall smallest value of S as the desired C.

3. Evaluation with simulated data

This evaluation was restricted to simulated data with unequal element gain and phase responses only. It was designed to show the adverse effects of unequal responses on elevation angle estimates calculated with a HRDF method and illustrate how calibration could alleviate these effects. The radar, target, and propagation parameters were chosen to produce results similar to those of the experimental evaluation in the next section.

3.1 Data Generation

The receive antenna was a vertical, uniform, linear array with N=8 elements spaced at a distance of 12.5 cm. It was centred at a height h_R=6.7 m above water. The operating frequency was 9.6 GHz, yielding a signal wavelength of λ=0.03125 m and an element spacing in wavelengths of d=4.0. The principal range of elevation angles was -7.2E to 7.2E.

The ideal snapshot $\mathbf{x}_m$ was generated using a flat earth model, Eq. (1), and

$$\theta_{Tm} = \tan^{-1}((h_{Tm}-h_R)/R_{Tm}) , \tag{13}$$

$$\theta_{Im} = \tan^{-1}((-h_{Tm}-h_R)/R_{Tm}) , \tag{14}$$

$$\alpha_{Tm} = \%\&\&\&\& \exp(j\phi_{Tm}) , \tag{15}$$

$$\alpha_{Im} = \rho\alpha_{Tm}\exp(j\delta_{\phi m}) , \tag{16}$$

$$\delta_{\phi m} = -2\pi\Delta_{Rm}/\lambda , \tag{17}$$

$$\Delta_{Rm} = 2h_{Tm}h_R/R_{Tm} , \tag{18}$$

$$\mathbf{a}(\theta) = (1,\exp[j2\pi d\sin\theta],\cong\cong\cong,\exp[j2\pi d(N-1)\sin\theta])^T . \tag{19}$$

The parameter h_{Tm} was the target height, R_{Tm} was the target range, SNR_T was the target SNR at the elements, ϕ_{Tm} was a random phase, ρ was the reflection coefficient at the water surface, Δ_{Rm} was the transit path difference between the target and image signals, and $\delta_{\phi m}$ was the phase correction for this difference. The ρ was assigned as

$$\rho = -0.9 , \tag{20}$$

corresponding to 0.92 dB attenuation and 180E phase change. In (19), the first element was the lowest element in the array and θ represented θ_{Tm} or θ_{Im}.

The measured snapshot $\mathbf{y}_m$ was generated with (2) and either

$$\mathbf{B} = \mathrm{diag}\{g_1,g_1,AAA,g_N\} \tag{21a}$$

or

$$\mathbf{B} = \mathrm{diag}\{g_1^*, g_2^*, AAA, g_N^*\} \ . \qquad (21b)$$

The g_n's were complex amplitudes of element gain and phase responses and had the values given in Table 1. These amplitudes were chosen to be the same as those calculated from the experimental data in the next section. The components of $\mathbf{e}_m$ in $\mathbf{y}_m$ were generated as uncorrelated complex Gaussian variates with zero mean and unit variance.

n	Gain*g_n*	Phase (°)
1	1.000	0.0
2	1.044	-14.0
3	0.988	-7.8
4	1.098	-16.6
5	0.978	-3.8
6	1.047	1.4
7	0.978	8.2
8	0.966	13.9

Table1. *Relative element gain $|g_n|$ and phase ang(g_n) responses in simulation.*

Three files were produced. File 1 used the **B** given by (21a) and had M=1971 snapshots. The target was a transmitter with SNR_T =30 dB at a fixed range R_{Tm}=8.0 km. It moved up from height h_{TI}=7.0 m to h_{TM}=992.0 m (θ_{TI}=0.00E, θ_{II}=-0.01E, θ_{TM}=7.02E, and θ_{IM}=-7.16E) while the snapshots were generated at intervals of 0.5 m. File 2 was generated with the same B and had M=451 snapshots. The target had SNT_T=20 dB and a fixed height h_{Tm}=46.0 m. It approached the radar from range R_{TI}=20.0 km to R_{TM}=2.0 km while the snapshots were generated at range intervals of 4.0 m. File 3 was generated with the **B** given by (21b). The other parameters were the same as those in File 2.

3.2 Calibration matrix

File 1 was used to calculate **C**. In Step 1, the assignments were Δ==0.00001 and i_{max}=400. In Step 7, the **C** calculated with $\mathbf{C}_0=\mathbf{I}_N$ was treated as the output of a coarse search. It was refined by repeating Steps 2 and 6 fifteen times. In each repetition, the new $\mathbf{C}_0$ was obtained by adding complex amplitudes with zero mean and 0.04 standard deviation to the **C** obtained in the coarse search. The step also included many other coarse searches followed by

refinements. In each coarse search, $\mathbf{C}_0$ was obtained by adding complex amplitudes with zero mean and 0.3 standard deviation to every coefficient of $\mathbf{I}_N$.

The **C** matrices at the end of these coarse-plus-refinement searches were essentially the same and were approximately diagonal. All those selected for further evaluation produced similar results. The values of S for these matrices were between 0.000407 and 0.000445. In the $\mathbf{C}_i$ with S=0.000407, all off-diagonal coefficients did not exceed 0.001 in magnitude and that the product $\mathbf{C}_i\mathbf{B}$ was an 8H8 identity matrix when only the first three decimal places were retained.

In the calculation with $\mathbf{C}_0=\mathbf{I}_N$, the Δ_i in Step 5 initially decreased monotonically from 0.2634584 at i=1 to 0.0000109 at i=181. Then, it fluctuated with amplitudes less than 0.0000001 and decreased further to less than 0.0000100 at i=198. The corresponding value of S decreased monotonically from 0.025769 at i=1 to 0.000435 at i=198. Refinement produced a new **C** with S=0.000434.

3.3 Elevation angle estimates

The TKSVD method [2,3] was used to calculate six candidate direction estimates from each snapshot in File 2, using a sixth order linear prediction filter and assuming that two signal sources were present. The two candidate direction estimates with the largest powers were identified as target and image elevation angle estimates. Fig. 1 shows the estimates, plotted as points, before (B, upper half) and after (A, lower) calibration. Also plotted are the target (solid line) and image (dashed line) tracks.

There are several notable observations. Firstly, the TKSVD estimates form two visually identifiable tracks: an upper track for the target, and a lower track for the image. Secondly, there is a bias in the TKSVD estimates before calibration, because the tracks produced by the TKSVD estimates are above the true tracks at ranges less than 5.0 km. This bias is not observable after calibration. Thirdly, before calibration, there are estimates that produce anomalous tracks between the true target and image tracks at ranges 4.4, 5.6, 7.9 and 13.2 km. After calibration, the anomalous tracks are replaced by horizontal tracks with approximately zero elevations. Finally, outside the 4.4, 5.6, 7.9 and 13.2 km regions, the individual estimates are closer to the true target and image tracks after calibration.

Fig. 2 was calculated with File 3, which was generated with the matrix **B** given by (21b). Only the elevation angle estimates before calibration are presented, because **C** could not be used to calibrate this file. Compared with the upper half of Fig. 1, both the bias in elevation angle estimates and the gradients of the anomalous tracks have changed signs. These sign changes show that equalisation of element phase responses is very important, because these responses play a dominant role in the generation of bias and anomalous tracks.

A study of the $\delta_{\phi m}$'s in Files 2 and 3 showed that the anomalous tracks were centred at ranges where the target and image signals had approximately the same phase at the centre of the array. After calibration, each snapshot close to these ranges produced one elevation angle estimate with θ.0.0E plus one estimate with θ.2.7E or -2.7E. The θ.∀2.7E estimates correspond to noise pole positions in the TKSVD method.

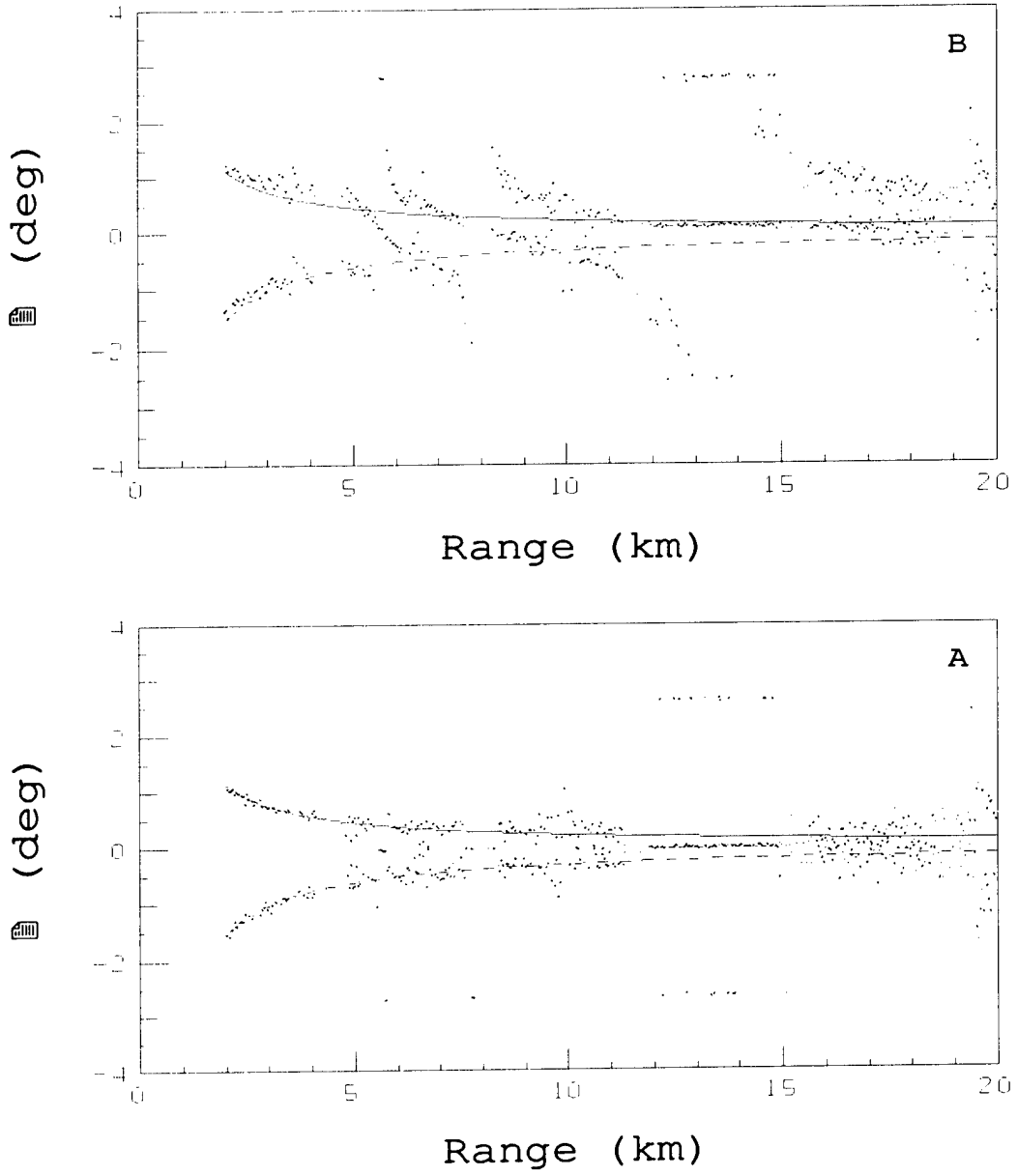

Figure 1. *TKSVD elevation angle estimates (points), target track (solid line), and image track (dashed line) obtained from simulated data File 2 before (B, upper half) and after (A, lower half) calibration.*

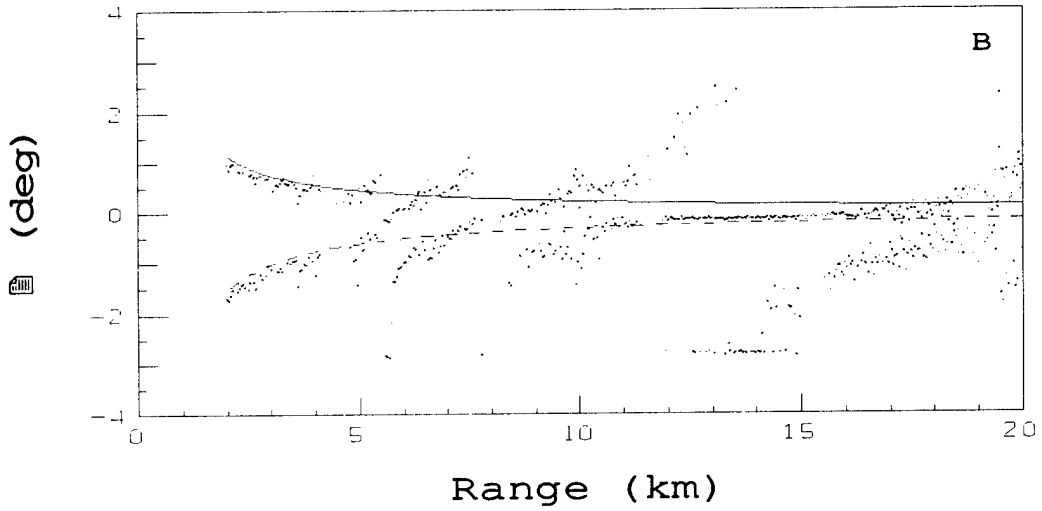

Figure 2. *TKSVD elevation angle estimates (points), target track (solid line), and image track (dashed line) obtained from simulated data File 3 before (B) calibration.*

4. Evaluation with experimental data

The experimental data sets in this evaluation were generated for the evaluation of LAT methods only. They were used to evaluate the calibration method because more suitable data were unavailable.

4.1 Experimental data

The experimental data were measured with an X-band LAT radar in 1981 by Standard Telecommunication Laboratories (STL) at the Fraser Gunnery Range, near Portsmouth, United Kingdom. This radar had separate vertically polarised transmit and receive antenna arrays mounted side by side on a pedestal that could be rotated about a vertical axis. Between them was an optical tracker to provide an independent measure of the target elevations. A detailed description of the experiment was given by Pearson and Waddoup [18] and a brief description is given in [4]. Here, it is sufficient to know that, like the set-up in the simulation evaluation, the transmit antenna operated at 9.6 GHz, the receive antenna was a vertical, uniform, linear array with N=8 elements spaced at a distance of d=4.0 wavelengths, and the principal range of target and image elevation angles is -7.2E to 7.2E.

This author had access to five data files. Each file was generated with a Hunter or Canbera aircraft flying towards the radar. It contained snapshots of the array element outputs as well as the aircraft ranges and elevations. Table 2 gives the file identifications, dates of measurement, aircraft types, number of array snapshots in the file, and the receive antenna heights. STL File 3 originally had 440 snapshots. Only the first 265 were retained, because the close-range snapshots had large range and elevation errors. Similarly, STL File 5 originally had 510 snapshots and only the first 405 were retained.

STL File	1	2	3	4	5
ID	250	252	311	312	313
1981 Date	June 18	June 18	June 25	June 25	June 25
Aircraft	Hunter	Hunter	Canberra	Canberra	Canberra
Snapshots	330	320	265	415	405
Nominal h_T (m)	46	46	61	61	61
Nominal h_R (m)	6.7	6.7	7.9	7.9	7.9
Bias (deg)	0.23	0.23	0.18	0.18	0.18

Table 2. *STL low-angle tracking data files*

4.2 Elevation estimates with uncalibrated data

The TKSVD method was used to calculate two elevation angle estimates from each snapshot in the files. The results obtained with STL Files 1 to 5 are plotted in the upper halves (B) of Figs. 3 to 7, respectively. Also plotted are the target tracks given by the optical tracker (solid lines). There are two notable observations. Firstly, the results look similar to those in the upper half of Fig. 1. Secondly, the bias in the TKSVD estimates depends on the date of the experiment.

The first observation is expected, because the parameters in the simulated data were chosen to produce results similar to the STL results. The second observation was first noted in [18], where it was stated that the exact reason was unknown.

The bias in a given file is denoted by θ_B and is given in Table 2. It is defined as the up-shift that must be applied to the optical track to make it fit the TKSVD target elevation angle estimates. The value is θ_B=0.23E for Files 1 and 2 generated on June 18 and θ_B=0.18E for Files 3 to 5 generated on 25.

4.3 Calibration matrix

Files 1 and 2 had the same bias and their optical tracks fitted the bias-removed TKSVD target elevation estimates very well. They were merged to produce a new file with 650 snapshots. This new file was used to calculate **C**, although Conditions 3 and 4 in Section 2.2 were not satisfied. In Step 1, the assignments were Δ==0.0001 and i_{max}=300. In Step 2, the target and image elevation angles were identified as the elevation angles in the target and image tracks, respectively. In Step 3, $\mathbf{Y}\hat{\mathbf{X}}^H$ was highly ill conditioned, because the target elevations did not exceed 1.5° and was well below the 7.2° upper limit of principal target elevation angles. Consequently, the $(\mathbf{Y}\hat{\mathbf{X}}^H)^{-1}$ in Eq. (9) was replaced by the Moore-Penrose pseudo-inverse calculated with the singular value decomposition method. Only the four largest singular values were not equated to zeroes, because this number produced the best results after calibration. Step 7 was omitted. In the result, Rank(**C**)=4 and **C** was not symmetric, not diagonal, and not even approximately diagonal.

The intermediate results showed that the Δ_i in Step 5 initially decreased monotonically from 0.73656 for i=1 to 0.00202 for i=63. Then, it fluctuated with amplitudes less than 0.00003 and decreased further to 0.00069 for i=300. The values of S was 0.03222 for i=1 and 0.00351 for i=2. It then increased slowly between i=2 and i=53 to 0.00462 before decreasing monotonically to 0.00436 for i=300. Between iterations i=2 and i=53, **C** gradually acquired the properties noted in Section 4.4 below. The decrease between i=53 and i=300 corresponded to a refinement of **C**.

4.4 Elevation estimates with calibrated data

The STL files were calibrated with **C**, using Eq. (5). The new TKSVD elevation angle estimates are plotted in the lower halves of Figs. 3 to 7. Evidently, the calibration has improved the accuracy of the estimates, improved the resolution of target and image elevation angles, suppressed the anomalous tracks between the target and image tracks, suppressed the bias in STL Files 1 and 2, and reduced the bias in Files 3 to 5.

The degree of improvement was better than expected, because the number of snapshots in the merged file was rather small, the SNR_T=s in snapshots were significantly lower than what one would get with a pilot source, and the largest target elevation angle was significantly below 7.2°. The bias in Files 3 to 5 were only reduced, because the bias in these files was different from the bias in the data used to calculate **C**.

4.5 Relative element gains and phases

The vector $\mathbf{g}(\theta)$, given by

$$\mathbf{g}(\theta) = \mathbf{C}^H\mathbf{a}(\theta)\,, \tag{22}$$

provides a measure of the relative gain and phase responses at the array elements for signal elevation θ. Table 1 gives the responses, relative to the first element, for θ=0.0E. These values were used in the generation of the simulated data used in Section 3.

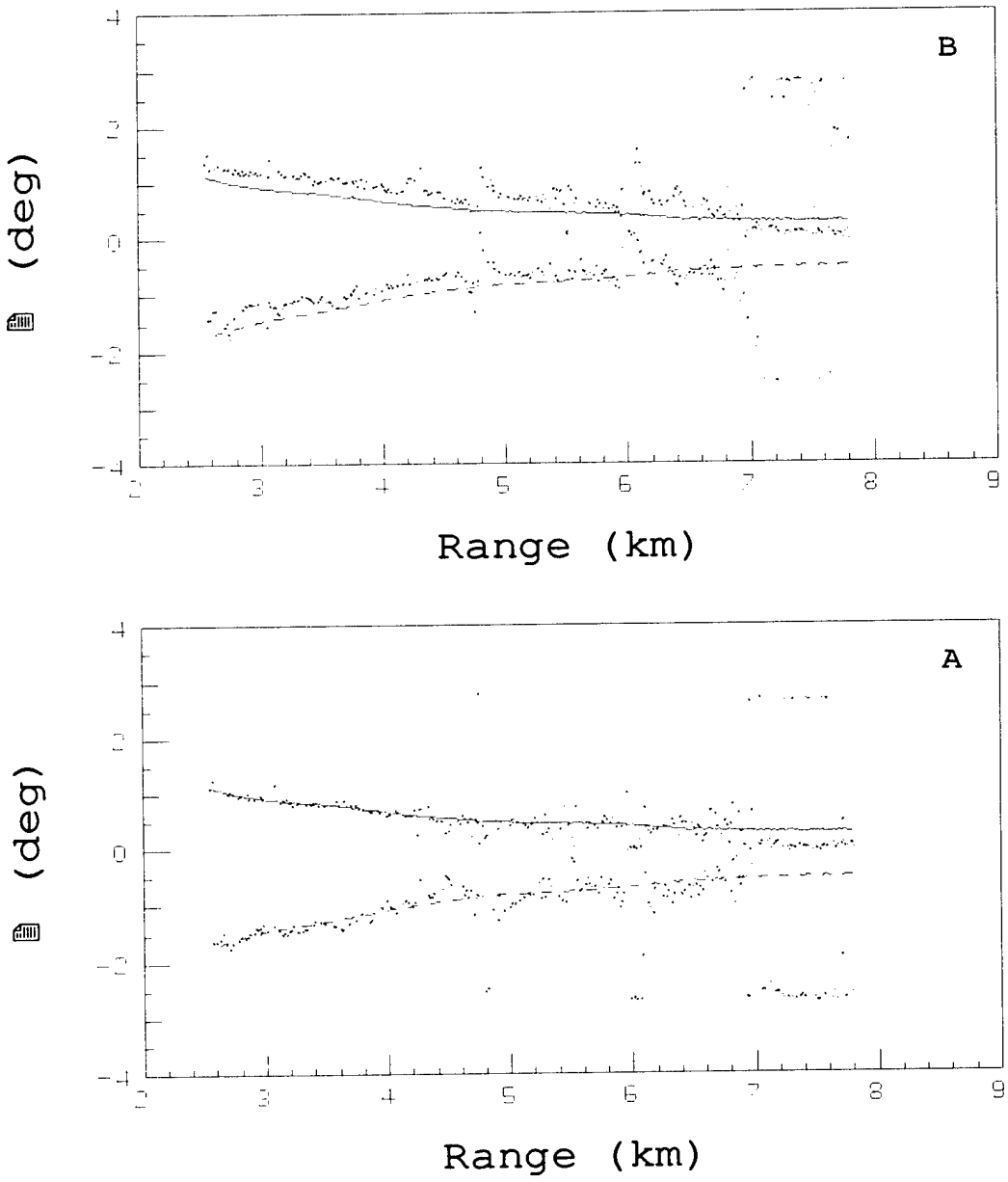

Figure 3. *TKSVD elevation angle estimates (points), optical target track (solid line), and image track (dashed line) obtained from STL File 1 before (B) and after (A) calibration.*

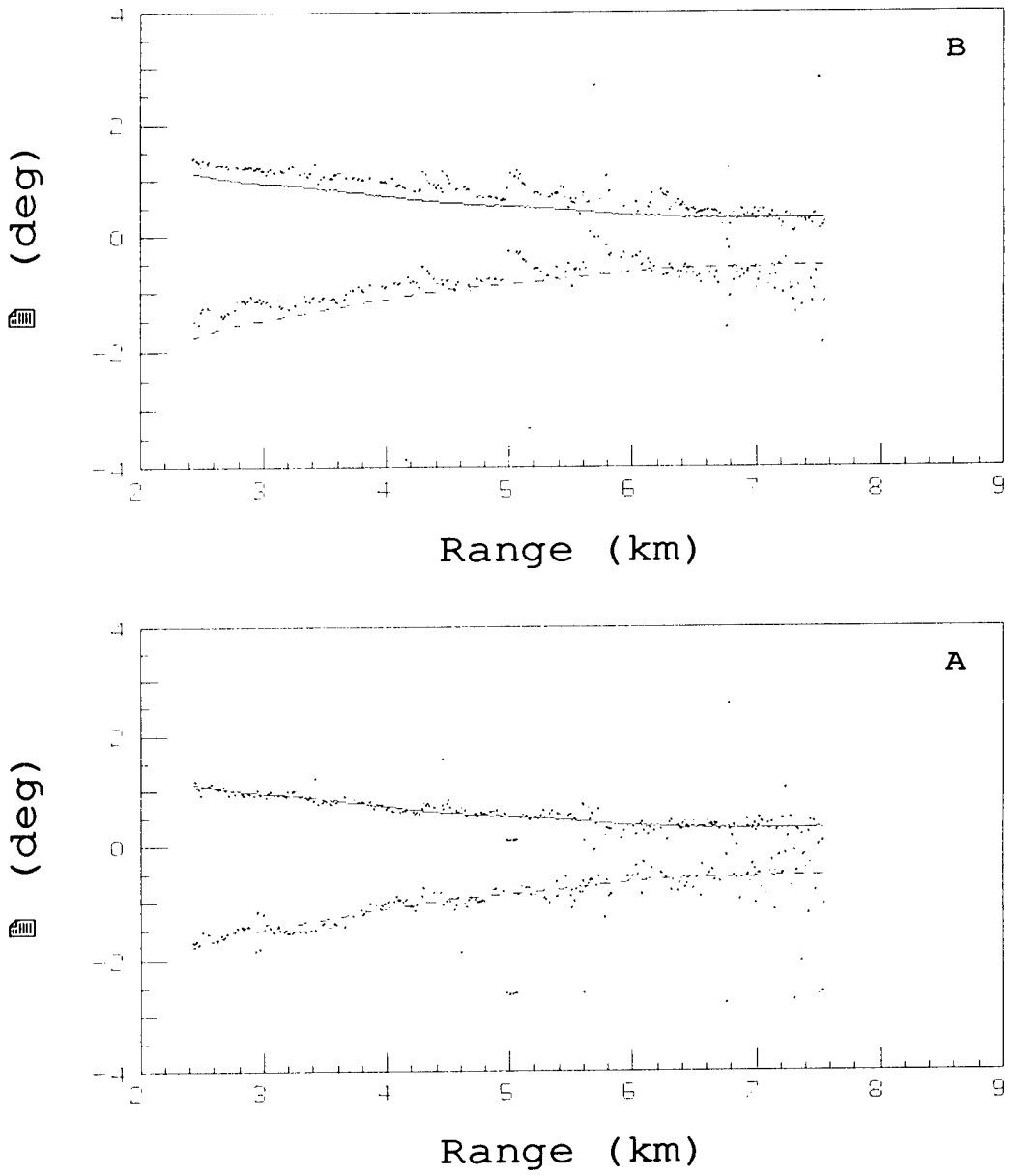

Figure 4. *TKSVD elevation angle estimates (points), optical target track (solid line), and image track (dashed line) obtained from STL File 2 before (B) and after (A) calibration.*

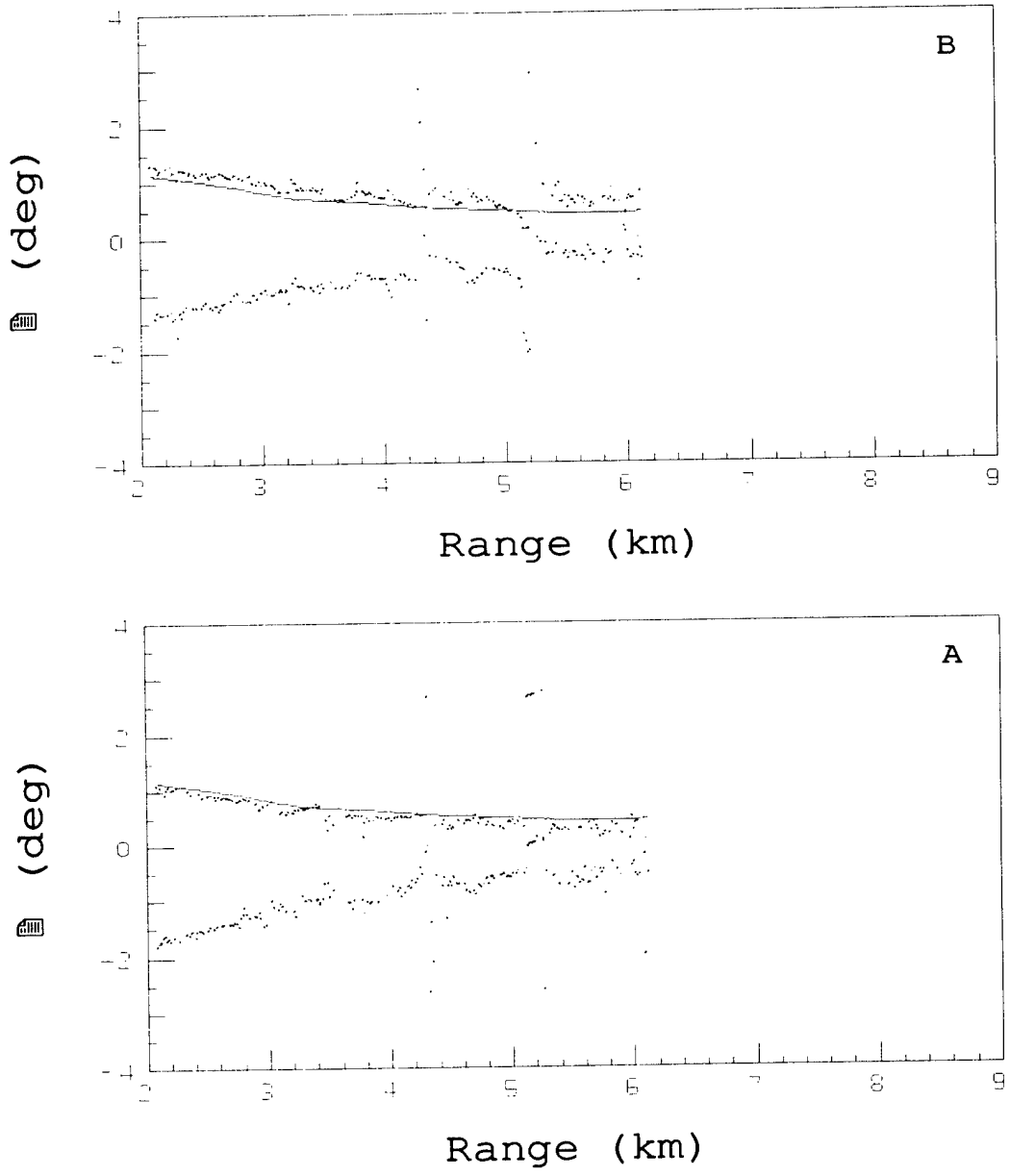

Figure 5. *TKSVD elevation angle estimates (points) and optical target track (solid line) obtained from STL File 3 before (B) and after (A) calibration.*

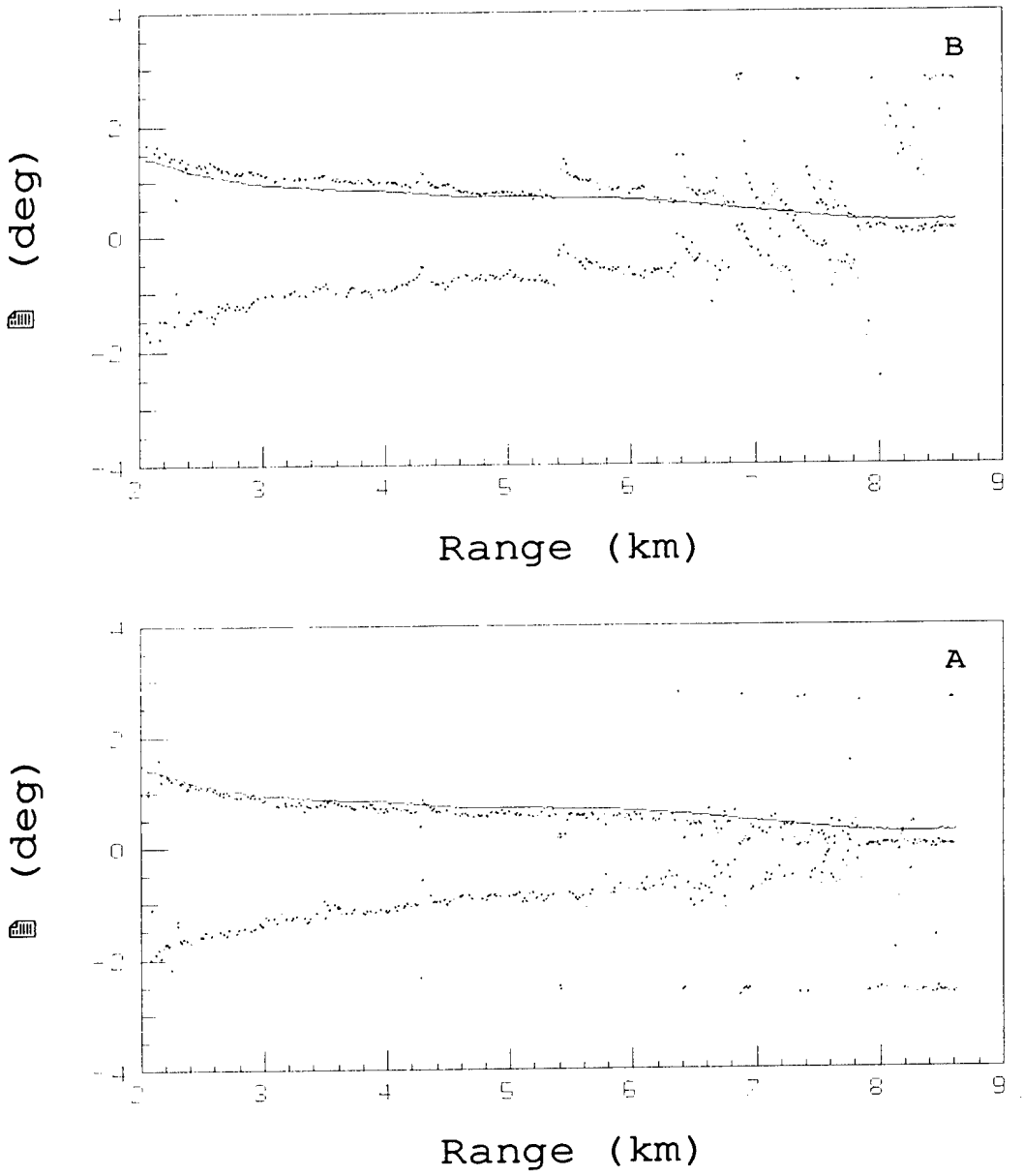

Figure 6. *TKSVD elevation angle estimates (points) and optical target track (solid line) obtained from STL File 4 before (B) and after (A) calibration.*

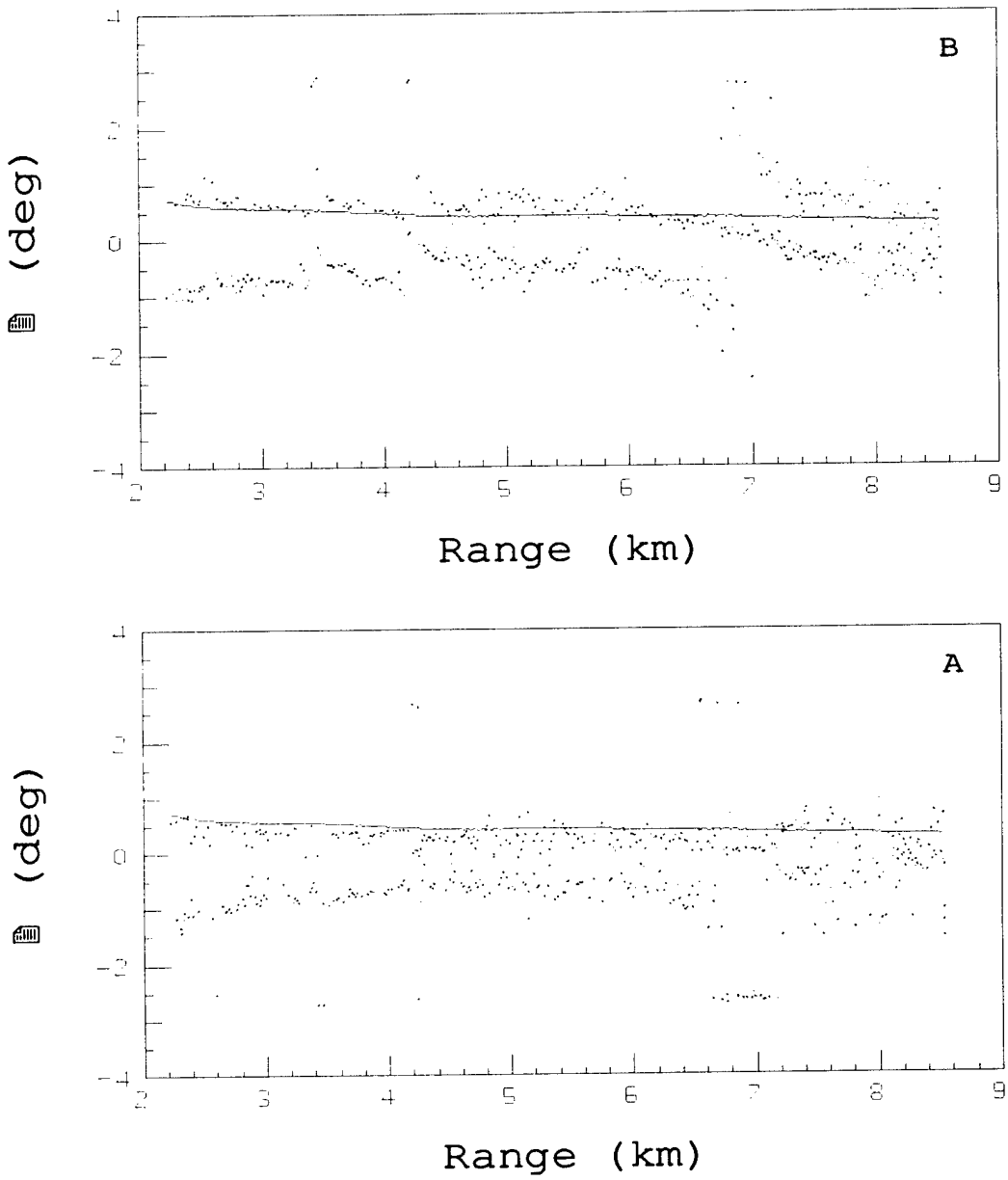

Figure 7. *TKSVD elevation angle estimates (points) and optical target track (solid line) obtained from STL File 5 before (B) and after (A) calibration.*

5. Conclusion

This author has described an in-situ method to calibrate an X-band antenna array for tracking low-elevation targets with HRDF methods. The simulation and experimental evaluations showed that the calibration (a) improved the accuracy of target elevation angle estimates calculated with the TKSVD method, (b) improved the resolution of target and image elevation angles, (c) suppressed a bias in elevation angle estimates, and (d) suppressed the anomalous tracks between the true target and image tracks.

6. References

1. R. O. Schmidt, "Multiple emitter location and signal parameter estimation", IEEE Transactions on Antennas and Propagation, Vol. AP-34, pp. 276-280, March 1986.

2. D.W. Tufts and R. Kumaresan, "Estimation of frequencies of multiple sinusoids: making linear prediction perform like maximum likelihood," Proceedings of the IEEE, Vol. 70, pp. 975-989, September 1982

3. D.W. Tufts and R. Kumaresan, "Estimating the angle of arrival of multiple plane waves," IEEE Transactions on Aerospace and Electronic Systems, Vol. AES-19, pp. 134-139, Jan. 1983

4. Haykin, S., Greenlay, T., and Litva, J., APerformance evaluation of the modified FBLP method for angle of arrival estimation using real radar multipath data,≅ IEE Proceedings, Vol. 132, Part F, pp. 159-174, June 1985.

5. Litva, J., AA new low-angle tracking technique,≅ Report 1335, Communications Research Centre, Ottawa, Canada, May 1980.

6. Rook, B.J. and Litva, AAn improved CHA algorithm for tracking low-angle target data,≅ Communications Research Centre, Department of Communications, Canada, Report No. 1356, April 1982.

7. Litva, J., AUse of highly deterministic model in signal-bearing estimation,≅ Electronics Letters, Vol. 25, No. 5, pp.346-348, March 1989.

8. Lo, T., and Litva, J., AUse of a highly deterministic multipath signal model in low-angle tracking,≅ IEEE Proceedings-F, Vol. 138, No. 2, pp. 163-171, April 1991.

9. Lo, T., Wong, T. and Litva, J., ANew technique for low-angle tracking,≅ Electronics Letters, Vol. 27, No. 6, pp. 529-531, March 1991.

10. Lo, T., and Litva, J., ALow-angle tracking using multifrequency sampled aperture radar,≅ IEEE Transactions on Aerospace and Electronic Systems, Vol. 27, No. 5, pp. 797-805, September 1991.

11. Bosse, E., Turner, R.M., and Lecours, M, >Tracking Swerling fluctuating targets at low altitude over the sea,= IEEE Transactions on Aerospace and Electronic Systems, Vol. 27, No. 5, pp. 806-822, September 1991.

12. Bosse, Eloi, Turner, Ross M., and Brookes, Daniel, AMUSIC and maximum likelihood using a refined propagation model: performance comparison for radar low-angle tracking,≅ Defence Research Establishment Ottawa, Ottawa, Canada, Report 1122, February 1992.

13. Bosse, E., Turner, R.M., and Riseborough, E.S., >Model-based multifrequency array signal processing for low-angle tracking,= IEEE Transactions on Aerospace and Electronic Systems, Vol. 31, No. 1, pp. 194-210, January 1995.

14. B. Friedlander, "A sensitivity analysis of the MUSIC algorithm," IEEE Transactions on Acoustics, Speech, and Signal Processing, Vol. 38, pp. 1740-1751, October 1990.

15. B. Friedlander, "Sensitivity analysis of the maximum likelihood direction-finding algorithm," IEEE Transactions on Aerospace and Electronic System, vol. 26, pp. 953-968, November 1990.

16. Hung, Eric K.L., AComputation of the coupling matrix among the elements of an array antenna," International Conference on Radar (Radar 94), pp. 703-706, Paris, France, May 1994.

17. Hung, Eric K.L., AMatrix-construction calibration method for antenna arrays,≅ IEEE Transactions on Aerospace and Electronic Systems, vol. 36, pp. 819-828, July 2000.

18. Pearson, A., and Waddoup, W.D., "Development and testing of an array signal processing tracking system," Standard Telecommunication Laboratories, United Kingdom, November 1981.

UNCLASSIFIED
SECURITY CLASSIFICATION OF FORM
(highest classification of Title, Abstract, Keywords)

DOCUMENT CONTROL DATA

(Security classification of title, body of abstract and indexing annotation must be entered when the overall document is classified)

1. ORIGINATOR (the name and address of the organization preparing the document. Organizations for whom the document was prepared, e.g. Establishment sponsoring a contractor's report, or tasking agency, are entered in section 8.)

Defence Research Establishment Ottawa
Department of National Defence
Ottawa, Ontario, Canada K1A 0Z4

2. SECURITY CLASSIFICATION (overall security classification of the document, including special warning terms if applicable)

UNCLASSIFIED

3. TITLE (the complete document title as indicated on the title page. Its classification should be indicated by the appropriate abbreviation (S,C or U) in parentheses after the title.)

In-situ calibration of an X-band antenna array for low-angle tracking with high-resolution direction-finding methods (U)

4. AUTHORS (Last name, first name, middle initial)

Hung, Eric K.L.

5. DATE OF PUBLICATION (month and year of publication of document)

6a. NO. OF PAGES (total containing information. Include Annexes, Appendices, etc.)

22

6b. NO. OF REFS (total cited in document)

18

7. DESCRIPTIVE NOTES (the category of the document, e.g. technical report, technical note or memorandum. If appropriate, enter the type of report, e.g. interim, progress, summary, annual or final. Give the inclusive dates when a specific reporting period is covered.)

Technical report

8. SPONSORING ACTIVITY (the name of the department project office or laboratory sponsoring the research and development. Include the address.)

Defence Research Establishment Ottawa
Department of National Defence
Ottawa, Ontario, Canada K1A 0K2

9a. PROJECT OR GRANT NO. (if appropriate, the applicable research and development project or grant number under which the document was written. Please specify whether project or grant)

05AB11

9b. CONTRACT NO. (if appropriate, the applicable number under which the document was written)

10a. ORIGINATOR'S DOCUMENT NUMBER (the official document number by which the document is identified by the originating activity. This number must be unique to this document.)

DREO TM 2000-122

10b. OTHER DOCUMENT NOS. (Any other numbers which may be assigned this document either by the originator or by the sponsor)

11. DOCUMENT AVAILABILITY (any limitations on further dissemination of the document, other than those imposed by security classification)

(X) Unlimited distribution
( ) Distribution limited to defence departments and defence contractors; further distribution only as approved
( ) Distribution limited to defence departments and Canadian defence contractors; further distribution only as approved
( ) Distribution limited to government departments and agencies; further distribution only as approved
( ) Distribution limited to defence departments; further distribution only as approved
( ) Other (please specify):

12. DOCUMENT ANNOUNCEMENT (any limitation to the bibliographic announcement of this document. This will normally correspond to the Document Availability (11). However, where further distribution (beyond the audience specified in 11) is possible, a wider announcement audience may be selected.)

UNCLASSIFIED
SECURITY CLASSIFICATION OF FORM

13. ABSTRACT (a brief and factual summary of the document. It may also appear elsewhere in the body of the document itself. It is highly desirable that the abstract of classified documents be unclassified. Each paragraph of the abstract shall begin with an indication of the security classification of the information in the paragraph (unless the document itself is unclassified) represented as (S), (C), or (U). It is not necessary to include here abstracts in both official languages unless the text is bilingual).

Presented in this report is an in-situ method to calibrate X-band antenna arrays designed to detect and track low-level missiles over water. These arrays are indispensable in ship defence, because they can operate in rainy and foggy conditions where atmospheric absorption is too high for the use of more accurate millimetre wave radars or optical devices.

The method uses a set of array snapshots to construct a calibration matrix for the antenna array. It incorporates the compensations for unequal gain and phase responses at the array elements, antenna tilt, mutual coupling among the elements, the effect of local structures, and small errors in element positions.

Simulation and experimental evaluations showed that the calibration (a) improved the accuracy of target elevation angle estimates obtained with a high-resolution direction-finding method, (b) improved the resolution of target and image elevation angles, (c) suppressed a bias in elevation angle estimates, and (d) suppressed some anomalous tracks between the true target and image tracks.

The calibration improves a ship's defence against low-level missiles.

14. KEYWORDS, DESCRIPTORS or IDENTIFIERS (technically meaningful terms or short phrases that characterize a document and could be helpful in cataloguing the document. They should be selected so that no security classification is required. Identifiers such as equipment model designation, trade name, military project code name, geographic location may also be included. If possible keywords should be selected from a published thesaurus. e.g. Thesaurus of Engineering and Scientific Terms (TEST) and that thesaurus-identified. If it is not possible to select indexing terms which are Unclassified, the classification of each should be indicated as with the title.)

X-band antenna array
In-situ calibration
Low-angle tracking
High-resolution direction-finding

UNCLASSIFIED
SECURITY CLASSIFICATION OF FORM